Research Square

Preprints are preliminary reports that have not undergone peer review.
They should not be considered conclusive, used to inform clinical practice,
or referenced by the media as validated information.

LcWRKY18 negatively regulates anthocyanin biosynthesis and is associated with high temperature-induced regreening in Loropetalum chinense var. rubrum

Anqi Huang
Hunan Agricultural Universit
Mingtong Ren
Hunan Agricultural Universit
Lili Xiang
Hunan Agricultural Universit
Yang Liu
Hunan Agricultural Universit
Jiaxuan Li
Hunan Agricultural Universit
Zhenkun Liao
Hunan Agricultural Universit
Lu Xu
Hunan Agricultural Universit
Donglin Zhang
University of Georgia
Nan Ma
Hunan Agricultural Universit
Xiaoying Yu
Hunan Agricultural Universit
Yanlin Li
liyanlin@huanue.edu.cn

Hunan Agricultural Universit

Research Article

Keywords: anthocyanin biosynthesis, high temperature, Loropetalum chinense var. rubrum, ornamental foliage shrub, WRKY transcription factor

Posted Date: May 15th, 2026

DOI: https://doi.org/10.21203/rs.3.rs-9482561/v1

License: This work is licensed under a Creative Commons Attribution 4.0 International License.
Read Full License

Additional Declarations: No competing interests reported.

Abstract

Loropetalum chinense var. *rubrum* is an important ornamental foliage shrub whose leaf coloration is highly sensitive to high temperature, often exhibiting high temperature-induced color fading due to reduced anthocyanin accumulation. However, the transcriptional mechanisms underlying this process remain poorly understood. In this study, we identified *LcWRKY18* as a transcription factor affected by high temperature and associated with color fading, based on the reference genomic data of *Loropetalum chinense* var. *rubrum* and the transcriptomic data under heat stress. Functional analyses showed that *LcWRKY18* negatively regulates anthocyanin accumulation, as its overexpression reduced anthocyanin accumulation, whereas its suppression promoted anthocyanin accumulation. Further multi-omics analyses revealed that *LcWRKY18* overexpression broadly suppressed the expression of structural genes in the phenylpropanoid and flavonoid biosynthetic pathways, leading to decreased levels of major anthocyanin metabolites, particularly cyanidin- and delphinidin-derived compounds. Consistently, dual-luciferase assays demonstrated that *LcWRKY18* directly inhibits the promoter activities of *LcPAL*, *LcANS* and *LcUFGT*. These results suggest that *LcWRKY18* acts as a negative regulator of anthocyanin biosynthesis that mediates high temperature-induced leaves color fading in *L. chinense* var. rubrum. This study provides new insight into the molecular basis of high-temperature-induced leaf color fading and offers a useful candidate gene for breeding ornamental germplasm with improved color stability under high temperature stress.

Highlights

• Identified *LcWRKY18* as a high temperature-responsive transcription factor associated with leaf color fading.

• *LcWRKY18* negatively regulates anthocyanin accumulation in *L. chinense* var. *rubrum*

• Integrated transcriptomic and metabolomic analyses revealed that *LcWRKY18* regulates anthocyanin metabolism by modulating the phenylpropanoid and flavonoid pathway.

• *LcWRKY18* suppresses anthocyanin biosynthesis by directly repressing key structural genes in the phenylpropanoid and flavonoid pathways, including.

1. Introduction

Colored-leaf plants are widely valued in landscape greening due to their distinctive foliage coloration, which greatly enhances ornamental appeal. However, increasing frequency of extreme weather events, particularly prolonged high-temperature conditions associated with global warming, has imposed significant abiotic stress on plants [1]. High temperature is a critical environmental factor affecting leaf pigmentation in colored-leaf species, often leading to color fading and a decline in ornamental quality, thereby limiting their landscape application [2].

Loropetalum chinense var. *rubrum*, a natural variant of Loropetalum in the Hamamelidaceae family [3], is a representative ornamental colored-leaf shrub. Its characteristic red foliage is primarily attributed to the accumulation of anthocyanins [4]. Previous studies have shown that leaves coloration in this species is mainly determined by anthocyanins derived from pelargonidin, cyanidin, and delphinidin [5,6]. Notably, high temperature induces a typical regreening phenotype in L. chinense var. rubrum, in which red leaves gradually lose pigmentation and turn green [5]. which is largely associated with a decline in anthocyanin accumulation[7–9]. These findings indicate that high temperature plays a pivotal role in regulating anthocyanin accumulation and leaf coloration in *L. chinense* var. *rubrum*. However, the molecular mechanisms underlying high temperature-induced anthocyanin reduction and leaf color fading remain largely unclear.

Anthocyanins are natural water-soluble pigments belonging to the flavonoid branch of polyphenolic compounds [10]. In addition to conferring attractive colors to flowers and fruits, they play important roles in stress adaptation by enhancing tolerance to adverse environments [11–16]. Anthocyanin biosynthesis originates from the phenylpropanoid pathway and involves a series of structural genes. Early biosynthetic genes (EBGs), including CHS, CHI, F3H, F3'H and F3'5'H, catalyze the formation of dihydroflavonols, whereas late biosynthetic genes (LBGs), including DFR, ANS/LDOX and UFGT, further convert these intermediates into anthocyanins [17]. In addition, anthocyanins can be modified by glycosylation, methylation and acylation and are transported into vacuoles for storage with the involvement of transport-related proteins such as GST [18,19]. Anthocyanin biosynthesis genes are largely controlled by the MYB-bHLH-WDR (MBW) transcriptional complex [20]. which regulates the expression of key structural genes and is evolutionarily conserved across plant species [21–25].

In addition to endogenous transcriptional regulation, anthocyanin accumulation is strongly influenced by environmental factors, including light, temperature, and water status. Among these, temperature is considered a critical determinant of anthocyanin stability and accumulation, with high temperature often leading to reduced anthocyanin content and color fading in plants. Environmental cues are known to modulate anthocyanin biosynthesis primarily by affecting the expression of structural genes and core regulatory factors such as MYB proteins. In addition to MYB factors, other transcription factors NAC, MADS-box, bZIP, WRKY and SPL also participate in anthocyanin regulation under environmental stimuli. For example, NAC and bZIP transcription factors can regulate anthocyanin accumulation by interacting with MYB proteins or integrating environmental signals, as exemplified by MdNAC42 and HY5-mediated regulatory pathways [26,27]. In recent years, Several WRKY proteins have been reported to either promote or repress anthocyanin accumulation in different species, suggesting their potential roles in linking environmental signals with secondary metabolites biosynthesis [28,29].

WRKY transcription factors are a large plant-specific family characterized by a conserved WRKYGQK motif and their ability to bind W-box cis-elements in target gene promoters, thereby regulating downstream gene expression [30,31]. Accumulating evidence indicates that WRKY proteins play important roles in plant responses to abiotic stresses, including drought, salinity, and temperature extremes, by modulating stress-responsive signaling pathways [32–39]. In addition to their roles in stress

responses, several WRKY transcription factors have been reported to participate in the regulation of anthocyanin biosynthesis in different plant species, including MdWRKY40 [40], MdWRKY71-L [41], MdWRKY1 [42], PpWRKY44 [43] ,LhWRKY44 [44],AtWRKY41 [21], These findings suggest that WRKY proteins may function as integrators of environmental signals and pigment metabolism. However, their specific roles in mediating anthocyanin biosynthesis under high temperature stress remain largely unclear.

In our previous work, 79 WRKY genes were identified and characterized in L. chinense var. rubrum and renamed *LcWRKY1-LcWRKY79* according to their chromosomal positions [45]. To clarify the regulatory role of WRKY genes in anthocyanin biosynthesis under high temperature stress, the expression patterns of 79 *LcWRKY* genes were systematically analyzed based on previous transcriptome data from high temperature-treated plants. And then a differentially expressed genes named *LcWRKY18* was screened as a candidate gene potentially involved in high temperature-induced anthocyanin reduction. In this study, *LcWRKY18* was functionally characterized through gene overexpression and silencing approaches, combined with transcriptomic-metabolomic analysis and molecular assays. Our results aim to clarify the role of *LcWRKY18* in regulating anthocyanin biosynthesis under high temperature stress and to provide new insights into the molecular mechanisms underlying leaf color variation in ornamental plants.

2. Materials and methods

2.1. Plant materials

Three Loropetalum cultivars, ‘Xiangnong Nishang’, ‘Xiangnong Fendai’ and ‘Hei Zhenzhu’ used in this study were obtained from the Engineering Research Center for Breeding and Utilization of Mid-subtropical Quality Ornamental Plants, Hunan Agricultural University. Nicotiana benthamiana plants for transient expression assays were cultivated in a growth chamber under controlled conditions: a temperature range of 22–25℃, a photoperiod of 16 h light / 8 h dark, LED light sources, and a relative humidity maintained between 55–65%. These conditions were implemented to ensure robust plant growth and stability of the transient expression system.

2.2Heat stress treatment conditions

For transcriptome sequencing in the previous stage of this study, three potted plants each of ‘Hei Zhenzhu’, ‘Xiangnong Fendai’ and ‘Xiangnong Xiangyun’ were subjected to high temperature in a growth chamber. Day/night temperatures were set at 40/33 C, with a 14-h light / 10-h dark photoperiod. LED lighting was used, the photosynthetic photon flux density was set at 30,000 lx, and relative humidity was maintained at 90%.

2.3Transcriptome data analysis

Raw read-count data obtained from transcriptome sequencing were normalized using the DESeq2 package in R. Size factors were calculated to correct sequencing-depth differences among samples and generate normalized count values. Differential expression analysis was then conducted with DESeq2 for

T0 vs T1, T0 vs T3, T0 vs T5, T0 vs T7, pCAMBIA1305-GFP vs pCAMBIA1305-*LcWRKY18*, and pTRV2-GFP vs *LcWRKY18* comparisons. Genes with |log2 fold change| >= 1 and false discovery rate (FDR) < 0.05 were considered differentially expressed.

2.4. RNA extraction and qRT-PCR analysis

Total RNA was extracted from roots, stems and leaves of 'Hei Zhenzhu', as well as from K599-transformed roots, using the FastPure Universal Plant Total RNA Isolation Kit (Vazyme) according to the manufacturer's instructions. High-quality RNA was reverse-transcribed into first-strand cDNA using the Vazyme reverse transcription kit and stored at -20°C for subsequent cloning and expression analyses.

Primers were designed using Primer3Plus and experimentally validated before use (Table 1). Loropetalum beta-actin was used as the internal reference gene. Each assay included three biological replicates and three technical replicates. Quantitative PCR was performed with the SYBR Green Pro Taq HS premix (Accurate Biology, AG11701), and relative expression levels of *LcWRKY18* and anthocyanin biosynthetic genes were calculated using the $2^{-\Delta\Delta CT}$ method.

2.5. Bioinformatic analysis of *LcWRKY18*

Candidate *LcWRKY* genes were first examined by qRT-PCR using cDNA from five high temperature time points as templates. Relative expression was calculated using the $2^{-\Delta\Delta CT}$ method with the T0 sample as the calibrator.

The physicochemical properties of *LcWRKY18*, including molecular weight and isoelectric point, were predicted using ExPASy ProtParam. Signal peptides were predicted with SignalP 4.1, transmembrane domains with TMHMM 2.0, and subcellular localization with WoLF PSORT. Secondary structure was predicted with SOPMA, and the protein structure was modeled using AlphaFold3.

Homologous proteins of *LcWRKY18* were searched using NCBI BLASTP. Sequences showing more than 50% similarity were aligned in DANMAN. A phylogenetic tree was constructed in MEGA7 using the neighbor-joining method with reported high temperature and anthocyanin-related WRKY proteins from other species. Cis-regulatory elements in the − 2kb promoter regions upstream of *LcWRKY* genes were analyzed using PlantCARE and visualized with TBtools [46].

2.6. Cloning of *LcWRKY18*

The coding sequence of *LcWRKY18* was retrieved from the L. chinense var. rubrum genome database. Gene-specific cloning primers (Table 1) were designed in Primer3Plus and synthesized by Tsingke Biotechnology (Beijing, China). Using cDNA from leaves of 'Xiangnong Nishang' as the template, the full-length coding sequence of *LcWRKY18* was amplified with a high-fidelity polymerase. The ligation products were transformed into Escherichia coli DH5a competent cells, and plasmids from positive colonies were extracted after sequence confirmation.

2.7. Subcellular localization of *LcWRKY18*

The pBI121-GFP vector was used for subcellular localization. The full-length CDS of *LcWRKY18* was amplified from pEASY-T1-*LcWRKY18* and inserted into pBI121 by homologous recombination after BamHI digestion. The resulting pBI121-*LcWRKY18* construct and the empty vector were introduced into Agrobacterium tumefaciens GV3101.

Positive Agrobacterium clones were cultured in medium containing 50 mg/L kanamycin and 50 mg/L rifampicin until OD_{600} reached 1.0. Cells were harvested, washed and resuspended in infiltration buffer (10 mM MES, 10 mM $MgCl_2$, 0.2 mM acetosyringone, pH 5.6) to an OD_{600} of 0.8, and then incubated in darkness for 3 h. The suspensions were infiltrated into the abaxial side of healthy N. benthamiana leaves with a 1-mL syringe. After 48 h of dark incubation, fluorescent signals around the infiltration sites were observed and photographed under a laser confocal microscope.

2.8. Transcriptional activation assay

To test self-activation activity and toxicity, the coding region of *LcWRKY18* was inserted into the BD vector through EcoRI and BamHI restriction sites. The resulting BD-*LcWRKY18* construct, the negative control (pGADT7-T + pGBKT7-Lam), and the positive control (pGADT7-T + pGBKT7-p53) were transformed into yeast strain Y2HGold and analyzed on selective media.

2.9. Vector construction and Agrobacterium rhizogenes-mediated root transformation

For overexpression, the verified pEASY-T1-*LcWRKY18* plasmid was used as a template, and seamless-cloning primers were designed according to the pCAMBIA1305-GFP vector map and *LcWRKY18* sequence. The vector was linearized with BamHI, and homologous recombination, transformation and colony screening were performed as described above.

For gene interference, a 300-bp fragment of *LcWRKY18* was selected using the VIGS tool in Sol Genomics Network, and primers containing SamI sites were designed according to the pTRV2 vector. Homologous recombination and bacterial transformation were performed as for the overexpression vector.

K599 A. rhizogenes competent cells stored at -80 ℃ were thawed and transformed with pCAMBIA1305-*LcWRKY18*, pTRV2-*LcWRKY18*, pTRV1, pTRV2 and pCAMBIA1305-GFP. Transformed cells were plated on selective medium and incubated at 28 ℃ for 2–3 d. Positive colonies were identified by PCR and cultured in TY medium supplemented with 50 mg/L kanamycin and 50 mg/L streptomycin to OD_{600} = 0.4.

One-year-old cuttings of ‘Hei Zhenzhu’ were used for root transformation. Lateral roots and fibrous roots were removed, leaving approximately 1 cm of the main root. Seedlings were immersed for 30 min in suspensions of pCAMBIA1305-GFP, pCAMBIA1305-*LcWRKY18*, pTRV2 or pTRV2-*LcWRKY18*; for VIGS treatment, pTRV2-derived cultures were mixed 1:1 with pTRV1 cultures. After inoculation, seedlings were planted in soil and 2 mL of the corresponding bacterial suspension was applied to the base of the stem. Plants were then maintained in a growth chamber.

Genomic DNA was extracted using the SteadyPure Plant Genomic DNA Extraction Kit (CTAB method, Accurate Biology, AG2106). PCR-based identification of transformed roots was carried out using primers specific for the rolB gene in the T-DNA region of K599, the GFP marker on pCAMBIA1305 or pTRV2, and *LcWRKY18*-specific fragments (Table 1). The expression levels of *LcWRKY18* in positive lines were further examined by qRT-PCR.

Root coloration was recorded photographically. Fresh, normally pigmented roots were washed with distilled water, mounted as temporary water slides using the potato-clamp method, and observed under a light microscope. Anthocyanin content was determined using the pH differential method.

2.10. Metabolomic sample preparation

Twelve root samples stored at -80℃ were freeze-dried and ground into powder. Powdered material was weighed and extracted with 0.5 mL of 50% methanol aqueous solution containing 0.1% HCl. Samples were vortexed for 5 min, ultrasonicated for 5 min, and centrifuged at 12,000 rpm for 3 min at 4 ℃. The extraction was repeated once, the supernatants were combined and filtered, and the resulting solutions were used for LC-MS/MS analysis of anthocyanin compounds.

Anthocyanin metabolites were analyzed using an ExionLC AD ultra-performance liquid chromatography system coupled with a QTRAP 6500 + tandem mass spectrometer (SCIEX, China).

2.11. Molecular docking analysis

Based on the amino acid sequence of *LcWRKY18* and the core promoter sequences of LcUFGT, LcPAL and LcANS, three-dimensional structures were predicted with AlphaFold3. Models with high pLDDT values were selected for docking analysis. Protein-DNA interactions were predicted using the local version of HDOCKlite v1.1, and the interfaces of the resulting complexes were further analyzed using PLIP [47]. Relevant interaction details were visualized in PyMOL.

2.12. Dual-luciferase assay

LcWRKY18 and the cloned promoter fragments of LcUFGT, LcPAL and LcANS were used as templates for In-Fusion cloning into pGreenII 0800-LUC-based reporter vectors and corresponding effector constructs. Recombinant plasmids were transformed into Agrobacterium and co-infiltrated into tobacco leaves. Firefly luciferase and Renilla luciferase signals were measured according to the standard dual-luciferase procedure, and promoter activity was expressed as the LUC/REN ratio.

2.13. Statistical analysis

All analyses were conducted using at least three biological replicates. Data processing was performed in Excel 2007. Figures were prepared using GraphPad Prism 9.5 and Adobe Photoshop 2023. Significant differences among treatments were evaluated using Student's t-test and one-way analysis of variance, and different lowercase letters indicate significant differences at $P < 0.05$.

Table 1
Primer sequences used in this study

Primer name	Primer sequence (5'-3')	Assay
LcWRKY18-QP-F	TGGATGCAGCGTTTAGGGTT	Quantitative Real-time PCR
LcWRKY18-QP-R	CTCTCGTGGTTGTGGACTCC	Quantitative Real-time PCR
β-actin-F	CCACAAGGCTTATTGATAGAAT	Quantitative Real-time PCR
β-actin-R	CAATGGTTGAACCTGAATACT	Quantitative Real-time PCR
LcCHS-F	ATGATTAAGAAGCGTTACA	Quantitative Real-time PCR
LcCHS-R	GTCTAGCATCCAATGAAG	Quantitative Real-time PCR
LcCHI-F	CATTAACGATTGGCTTCT	Quantitative Real-time PCR
LcCHI-R	CCTATGATTGACTCCAGTA	Quantitative Real-time PCR
LcPAL-F	CTGAAGGGGAGTCATTTGGAAG	Quantitative Real-time PCR
LcPAL-R	TCCATCACCCACTCACTACTC	Quantitative Real-time PCR
LcDFR-F	TGCTAAGACATCGGCTGAGAAA	Quantitative Real-time PCR
LcDFR-R	TCAACGCTGGGAGTCCTGAA	Quantitative Real-time PCR
LcANS-F	CTATACTGAGGCAACAAG	Quantitative Real-time PCR

Note: lowercase letters indicate gene-specific lowercase bases where applicable.

Primer name	Primer sequence (5'-3')	Assay
LcANS-R	GTCTTCCTTCTTCTAAGC	Quantitative Real-time PCR
LcUFGT-F	AAGCAAGCGGTGTAACAT	Quantitative Real-time PCR
LcUFGT-R	CAAGGCACTACCATTCCAT	Quantitative Real-time PCR
LcWRKY18-F	ATGGTCTCCACTGAAAATTTTGG	Gene clone
LcWRKY18-R	TTAAGAAGAAGAAGAGCGAGAGGG	Gene clone
pBI121-LcWRKY18-F	GGACTCTAGAGGATCCATGGTCTCCACTGAAAATTTTGGCT	Subcellular localization
pBI121-LcWRKY18-R	GACCACCCGGGGATCCAGAAGAAGAAGAGCGAGAGGGAG	Subcellular localization
pCAMBIA-1305-LcWRKY18-F	CACGGGGGACGGATCCATGGTCTCCACTGAAAATTTTGGCT	Overpression
pCAMBIA-1305-LcWRKY18-R	CTTTGTAGTCGGATCCAGAAGAAGAAGAGCGAGAGGGAG	Overpression
pTRV2-LcWRKY18-F	TCCCCATGGAGGCCTATGGTCTCCACTGAAAATTTTGGC	Gene silencing
pTRV2-LcWRKY18-R	AAGGTTACCGAATTCTCTAACTCCGATTTCGTTCTAAATGC	Gene silencing
rolB-F	GCCAGCATTTTTGGTGAACT	detection
rolB-R	GGCACTGAACTTGCCGTTAT	detection
GFP-F	CTGGTCGAGCTGGACGG	detection
GFP-R	CTGGGTGCTCAGGTAGTGG	detection

Note: lowercase letters indicate gene-specific lowercase bases where applicable.

Primer name	Primer sequence (5'-3')	Assay
BD-LcWRKY18-F	CATGGAGGCCGAATTCATGGTCTCCACTGAAAATTTTGGCT	verification
BD-LcWRKY18-R	GCAGGTCGACGGATCCTTAAGAAGAAGAAGAGCGAGAGGGAGC	verification
pCAMBIA-1300-LcWRKY18-F	CCAAATCGACTCTAGAATGGTCTCCACTGAAAATTTTGGC	Overpression
pCAMBIA-1300-LcWRKY18-R	GCAGAAGCTTTCTAGAAGAAGAAGAAGAGCGAGAGGG	Overpression
pGreenII 0800-F-48540A	CGGTATCGATAAGCTggccaatgacaccaaatcct	Dual-luciferase assay
pGreenII 0800-R-48540A	TAGAACTAGTGGATCtaacctaaaatacctacgatgtcataacaaattca	Dual-luciferase assay
pGreenII 0800-F-48540B	CGGTATCGATAAGCTttacaaacctacaagtgagcctattcacg	Dual-luciferase assay
pGreenII 0800-R-48540B	TAGAACTAGTGGATCgggacgtgacaacccccag	Dual-luciferase assay
pGreenII 0800-F-12653	CGGTATCGATAAGCTtatttaactagtcgccgccctgg	Dual-luciferase assay
pGreenII 0800-R-12653	TAGAACTAGTGGATCacttctactctccctcttcttatttatgttttatttttttagttaaaaaa	Dual-luciferase assay
pGreenII 0800-F-44833	CGGTATCGATAAGCTtagtgcatagttatcagaaccgaacgg	Dual-luciferase assay
pGreenII 0800-R-44833	TAGAACTAGTGGATCtattggttgattgaccttctttattttaagaaaaggatcgt	Dual-luciferase assay

Note: lowercase letters indicate gene-specific lowercase bases where applicable.

3. Results

3.1. Expression profiles of anthocyanin pathway genes and LcWRKY family members in different cultivars under high temperature

Based on transcriptome count data, differential expression analyses were performed for samples collected at different high temperature stages. In ‘Hei Zhenzhu’, a large number of *LcWRKY* genes were differentially expressed during the middle stage of high temperature (T1, T3 and T5), whereas a different response pattern was observed in ‘Xiangnong Fendai’ (Fig.S1A,B).

Using the differential-expression results together with transcript abundance data, high temperature maps were constructed to visualize the expression patterns of *LcWRKY* genes in ‘Hei Zhenzhu’ and‘Xiangnong Fendai’under high temperature. In ‘Hei Zhenzhu’, *LcWRKY18* displayed a highly characteristic expression profile and was strongly associated with the high temperature regreening phenotype (Fig. 1A,B).

Nine genes, namely *LcWRKY13*, *LcWRKY18*, *LcWRKY21*, *LcWRKY30*, *LcWRKY36*, *LcWRKY39*, *LcWRKY46*, *LcWRKY49* and *LcWRKY74*, were preliminarily selected based on differential-expression and expression-pattern analyses. qRT-PCR verification showed that the expression trend of *LcWRKY18* was highly consistent with the transcriptome data, supporting its selection as the major candidate gene for further study(Fig. 2A,B).

3.2. Bioinformatic analysis of *LcWRKY18*

The coding sequence of *LcWRKY18* was 534 bp in length according to the Loropetalum genome database. Using cDNA from leaves of ‘Xiangnong Nishang’ as the template, the full-length CDS was successfully amplified, and agarose gel electrophoresis showed a single clear band of the expected size(Fig.S2).

Comprehensive bioinformatic analysis showed that the *LcWRKY18* protein consists of 177 amino acids and has the typical features of a WRKY transcription factor. Prediction using ProtParam indicated a theoretical molecular mass and isoelectric point consistent with a small regulatory protein. SignalP predicted that *LcWRKY18* lacks a signal peptide, indicating that it is not a secreted protein. TMHMM analysis further showed that it has no transmembrane domain(Fig.S3A,B).

Secondary-structure prediction indicated that *LcWRKY18* is mainly composed of random coils, together with a small proportion of alpha-helices and extended strands. Structural modeling supported the presence of a typical WRKY DNA-binding domain(Fig.S3C,D).

Phylogenetic analysis revealed that *LcWRKY18* clustered with several reported WRKY proteins involved in stress responses and anthocyanin regulation in other species, including *MdWRKY40* [40], *PpWRKY44* [43], *LhWRKY44* [44], *AtWRKY41* [21]and *ZjWRKY18* [48] (Fig. 3A). Multiple sequence alignment indicated that *LcWRKY18* contained the conserved WRKYGQK motif and a typical C2H2-type zinc-finger structure, consistent with the defining features of WRKY transcription factors [30,31] (Fig. 3B).

Using cDNA from leaves, stems and roots of the cultivars ‘Hei Zhenzhu’ and ‘Xiangnong Xiangyun’, qRT-PCR showed that LcWRKY18 was expressed in all tested tissues but exhibited clear tissue specificity and cultivar-dependent variation. The relatively high expression in pigmented tissues suggested a close relationship with pigment metabolism and stress responses(Fig.S4).

3.3. Subcellular localization and transcriptional activation of *LcWRKY18*

To determine the intracellular localization of *LcWRKY18*, the pBI121-*LcWRKY18* fusion vector was transiently expressed in tobacco leaves. Confocal microscopy showed that the GFP signal of the fusion protein was distributed in both the nucleus and cytoplasm, whereas the control showed ubiquitous fluorescence, indicating that *LcWRKY18* is a nucleocytoplasmic protein(Fig. 4).

In yeast, pGBKT7-*LcWRKY18* grew normally on SD/-Trp/-Leu medium, suggesting that the bait construct was not toxic. The transformed yeast strains were then transferred to highly selective media to evaluate self-activation. The results indicated that *LcWRKY18* did not show obvious self-activation activity under the tested conditions(Fig.S5).

3.4. Functional verification of *LcWRKY18* by transient overexpression and interference

K599-mediated transformation successfully generated transgenic roots in ‘Hei Zhenzhu’. PCR analysis revealed the presence of the rolB, gfp, and *LcWRKY18* genes in the transgenic roots (with no signals detected in the water and WT controls) (Fig. 5A,B). qRT-PCR assays demonstrated that the vector pCAMBIA1305-*LcWRKY18* upregulated the expression of the target gene in ‘Heizhenzhu’ by 4.17-fold compared to the empty vector, while the vector pTRV2-*LcWRKY18* downregulated its expression to 0.21-fold of the empty vector(Fig. 5C,D). Collectively, the results from PCR and qRT-PCR verified the successful establishment of the target gene overexpression and interference systems.

Phenotypic observations showed that in the ‘Hei Zhenzhu’ cultivar, the roots of *LcWRKY18* overexpression lines had significantly reduced anthocyanin content, which was decreased to 0.56-fold of that in the wild-type (WT) and empty vector controls. In contrast, RNA interference-mediated silencing of *LcWRKY18* did not result in a significant fading phenotype; instead, it promoted pigment accumulation, with the anthocyanin content increased to 2.24-fold of the WT level(Fig. 5E,F,G).The expression levels of structural genes involved in the anthocyanin biosynthesis pathway in the roots of transgenic plants were analyzed. The results showed that, compared with the control roots transformed with the empty pCAMBIA1305 vector, the expression levels of the anthocyanin biosynthetic structural genes PAL, CHS, CHI, DFR, ANS, and UFGT in the roots of the pCAMBIA1305-*LcWRKY18* overexpression line decreased to 0.52-fold, 0.53-fold, 0.83-fold, 0.42-fold, 0.34-fold, and 0.60-fold of the control levels, respectively. In contrast, compared with the control roots transformed with the empty pTRV2-GFP vector, the expression

levels of the same genes in the roots of the pTRV2-*LcWRKY18* silencing line increased to 1.64-fold, 3.81-fold, 3.53-fold, 6.53-fold, 4.99-fold, and 2.12-fold of the control levels, respectively(Fig. 5H,I).

These results suggest that *LcWRKY18* acts as a negative regulator of anthocyanin biosynthesis, functioning to repress the accumulation of anthocyanins.

3.5. Transcriptomic and metabolomic analyses of *LcWRKY18* transgenic materials

To further investigate how *LcWRKY18* regulates color change in *L. chinense* var. *rubrum*, transcriptome sequencing was performed on 15 transgenic samples. Principal component analysis showed clear separation among the different groups, indicating good repeatability and distinct transcriptional states among overexpression, interference and control samples(Fig. 6A).

Based on time-series analysis, the gene expression profiles of WT, pCAMBIA1305-GFP, pCAMBIA1305-LcWRKY18, pTRV2-GFP, and pTRV2-LcWRKY18 were clustered into 10 modules. Significant differences in expression levels were observed among different sample groups within these modules, suggesting that LcWRKY18 may exert its biological functions by regulating gene expression(Fig. 6B). Differential expression analysis was performed for four comparison groups: WT vs pCAMBIA1305-LcWRKY18, pCAMBIA1305-GFP vs pCAMBIA1305-LcWRKY18, WT vs pTRV2-LcWRKY18, and pTRV2-GFP vs pTRV2-LcWRKY18. The results revealed that the WT vs pCAMBIA1305-LcWRKY18 comparison contained 10,042 differentially expressed genes (DEGs), including 6,796 up-regulated and 3,246 down-regulated genes; the pCAMBIA1305-GFP vs pCAMBIA1305-LcWRKY18 comparison contained 5,076 DEGs, including 1,624 up-regulated and 3,452 down-regulated genes; the WT vs pTRV2-LcWRKY18 comparison contained 9,560 DEGs, including 5,959 up-regulated and 3,601 down-regulated genes; and the pTRV2-GFP vs pTRV2-LcWRKY18 comparison contained 4,103 DEGs, including 3,783 up-regulated and 320 down-regulated genes(Fig. 6C).

GO enrichment analysis indicated that differentially expressed genes were mainly enriched in phenylpropanoid metabolic process, phenylpropanoid biosynthetic process, lignin metabolic process, lignin biosynthetic process and response to chitin, among others(Fig. 6D). KEGG enrichment further showed significant enrichment in flavonoid biosynthesis, monoterpenoid biosynthesis, phenylpropanoid biosynthesis, starch and sucrose metabolism, and phenylalanine metabolism. These results suggested that *LcWRKY18* broadly affects secondary-metabolism-related pathways(Fig. 6E).

Transcriptome data further showed that overexpression or interference of *LcWRKY18* significantly altered the expression of multiple genes involved in the phenylpropanoid and flavonoid pathways, including key structural genes associated with anthocyanin biosynthesis.

To investigate the role of *LcWRKY18* in flavonoid metabolism more deeply, LC-MS/MS-based metabolomic profiling was performed on overexpression and interference materials. The results showed that *LcWRKY18* markedly affected the accumulation of various anthocyanin metabolites. In particular,

overexpression of *LcWRKY18* significantly inhibited the accumulation of cyanidin- and delphinidin-related compounds, whereas interference lines showed the opposite trend(Fig. 7). The heat map of anthocyanin metabolites clearly illustrated the differential accumulation pattern among the transgenic materials.

3.6. *LcWRKY18* represses the promoter activities of *LcUFGT*, *LcPAL* and *LcANS*

Based on the *Loropetalum chinense* var. *rubrum* genome database, the − 2000 bp DNA sequences upstream of the ATG start codon for six genes—*LcPAL*, *LcCHS*, *LcCHI*, *LcDFR*, *LcANS*, and *LcUFGT*—were retrieved as candidate promoter regions. These promoter sequences were subsequently submitted to the PlantCARE online analysis tool for cis-acting element prediction and analysis. Notably, multiple WRKY transcription factor binding sites (W-box elements) were identified in the promoters of *LcPAL*, *LcANS*, and *LcUFGT*, suggesting that these genes may be regulated by WRKY family transcription factors.

Results from overexpression and VIGS/interference experiments indicated that *LcWRKY18* may regulate structural genes involved in anthocyanin biosynthesis. Therefore, promoter regions of *LcUFGT*, *LcPAL* and *LcANS* were cloned from 'Xiangnong Nishang', and cis-element analysis revealed the presence of W-box motifs in these promoter fragments(Fig. 8A).

To further determine whether LcWRKY18 directly regulates the expression of *LcUFGT*, *LcPAL*, and *LcANS* genes, we performed a LUC transient expression assay in Nicotiana benthamiana. The pCAMBIA1300 vector harboring the *LcWRKY18* gene was used as the effector vector, while the pGreenII0800 LUC vector carrying the promoter sequences of *LcUFGT*, *LcPAL*, and *LcANS* was used as the reporter vector(Fig. 8B).

Dual-luciferase assays showed that co-expression of *LcWRKY18* significantly reduced the activities of the *LcUFGT*, *LcPAL* and *LcANS* promoters relative to controls. These results support the conclusion that *LcWRKY18* functions as a transcriptional repressor of key structural genes in the anthocyanin biosynthetic pathway(Fig. 8C).

Based on the amino acid sequence of *LcWRKY18* and the promoter sequences of *LcUFGT*, *LcPAL*, and *LcANS*, structure prediction was performed using AlphaFold3. The top-ranked structure was selected as the experimental model based on the pLDDT score. The PLIP interaction analysis platform was employed to comprehensively describe and systematically analyze the binding interfaces(Fig. 8D).

4. Discussion

WRKY transcription factors participate extensively in plant development, stress adaptation and specialized metabolism. Since the first WRKY protein SPF1 was cloned from sweet potato [49], large numbers of WRKY genes have been identified in Arabidopsis [50], rice [51] and maize [52]. Accumulating evidence shows that WRKY proteins function in seed dormancy and germination [53,54], root development [55–57], pollen development [58], floral morphogenesis [59], and responses to diverse

biotic and abiotic stresses, including high temperature [34,36,60,61]. Previous studies have identified a total of 79 *LcWRKY* genes in the *Loropetalum chinense* var. *rubrum* genome[45], which is approximately the same as the 74 members found in the model plant *Arabidopsis thaliana*[62]. Previous research has shown that *Arabidopsis thaliana* has undergone at least two whole-genome duplication events, which have contributed to the rapid expansion of its gene families[63,64].In the present study, *LcWRKY18* was identified from high temperature transcriptome datasets of *L. chinense* var. *rubrum* as a candidate gene associated with anthocyanin metabolism and regreening, and its functional analysis suggested that it acts as a negative regulator of anthocyanin accumulation under high temperature.

WRKY family members exhibit significant differential responses to heat stress among different plant species. For instance, in *Lilium longiflorum*, 62 *LdWRKY* genes were identified to be differentially expressed under heat stress, with 51 genes up-regulated and 11 genes down-regulated[65]; in contrast, in *Phoenix dactylifera*, 7 *PdWRKY* genes were up-regulated while 10 genes showed down-regulation[66].Through heat stress treatment of two *Loropetalum chinense* var. *rubrum* varieties, ‘Hei Zhenzhu’ and ‘Xiangnong Fendai’, it was observed that the number of differentially expressed members of the *LcWRKY* family and their temporal distribution exhibited obvious temporal dynamics. In ‘Hei Zhenzhu’, the largest number of differentially expressed genes was identified at the T0 vs T3 stage, whereas no differentially expressed genes were found at the T0 vs T7 stage. In ‘Xiangnong Fendai’, the number of differentially expressed genes gradually increased with the duration of heat stress, reaching 4 at the T0 vs T7 stage.In potato (*Solanum tuberosum*), the expression level of *StWRKY75* shows a significant difference between the heat-sensitive variety ‘Atlantic’ and the heat-tolerant variety ‘Desiree’, and this difference is directly related to the thermotolerance of the varieties[67].Meanwhile, the co-responsive genes of the two varieties were mainly concentrated at the T0vsT3 and T0vsT5 stages, indicating that 3–5 days after heat stress constitutes the critical phase for the *LcWRKY* gene family to exert its regulatory functions. The differences in the *LcWRKY* expression patterns between the two varieties are highly correlated with the stability of their leaf colors, suggesting that individual *LcWRKY* members may play important roles in the color stability of *Loropetalum chinense* var. *rubrum* under heat stress by regulating the anthocyanin metabolic pathway.

Cis-acting elements form the structural basis for transcription factors to respond to upstream signals and regulate downstream target genes. In the study of the WRKY gene family in *Phoenix dactylifera*, the promoter regions are rich in a variety of cis-elements related to abiotic stress responses, such as ABRE [66].Analysis of the promoter regions of *LcWRKY* genes in *Loropetalum chinense* var. *rubrum* revealed that all members contain elements related to heat stress responses, primarily including the Antioxidant Response Element (ARE), G-box element and Abscisic Acid Response Element (ABRE)[68,69] (Fig. 2E).

Sequence alignment and phylogenetic analysis confirmed that *LcWRKY18* contains the conserved WRKY domain and belongs to the canonical WRKY family [30,31]. The close relationship between *LcWRKY18* and reported anthocyanin-related WRKY proteins from other species suggests partial functional conservation. In addition, qRT-PCR showed that *LcWRKY18* exhibited clear tissue specificity in different cultivars.As key regulatory hubs in the secondary metabolic network, WRKY transcription factors are

involved in the regulation of biosynthesis for secondary metabolites such as flavonoids and terpenoids.In jujube, *ZjWRKY18* positively regulates triterpenoid accumulation and enhances salt tolerance [48]. These observations support the view that *LcWRKY18* genes may participate in both secondary metabolism and stress adaptation in different plant species.

The Agrobacterium rhizogenes-mediated hairy-root system provided an effective platform for rapid functional verification in L. chinense var. rubrum. Overexpression of *LcWRKY18* caused obvious fading of root color and a marked reduction in anthocyanin content, whereas interference of *LcWRKY18* had the opposite effect. The regulatory mechanisms underlying the role of WRKY transcription factors in anthocyanin biosynthesis are complex and diverse.In pear, *PyWRKY26* regulates the synthesis and transport of anthocyanins by targeting the promoter of *PyMYB114*[70]; in kiwifruit, *AcWRKY44* interacts with *MYBC1* to be involved in the regulation of the proanthocyanidin and anthocyanin biosynthetic pathways[71]. However, some WRKY members have been confirmed to possess transcriptional repression activity. In Arabidopsis thaliana, *AtWRKY31* has been identified as a transcriptional repressor [72]; *AtWRKY61* also exhibits transcriptional repression activity, where it binds to the W-box in the promoter of *ALMT1* to inhibit its expression[73]. In lily, although *LhWRKY44* has been confirmed to positively regulate anthocyanin biosynthesis, the same regulatory network also contains *LhHB4*, an HD-Zip transcription factor containing an EAR repression motif, which negatively regulates anthocyanin accumulation by suppressing the expression of *LhWRKY44* and *LhMYBSPLATTER* [74].Subcellular localization showed that *LcWRKY18* was distributed in both the nucleus and cytoplasm. This finding is inconsistent with the nuclear localization results of WRKY proteins reported in most studies. Such differences in localization may reflect the functional diversity of WRKY transcription factors. Studies have shown that WRKY transcription factors can sense signals in the cytoplasm and, in response to stimuli, be translocated into the nucleus to exert their regulatory functions.[75].

As plant-specific regulators, WRKY transcription factors play complex regulatory roles in the flavonoid metabolic network. Previous studies have demonstrated that WRKY transcription factors are involved in the regulation of anthocyanin and proanthocyanidin accumulation by directly targeting key structural enzyme genes in the flavonoid biosynthetic pathway [76]. Meanwhile, WRKYs act as regulatory hubs to integrate multiple developmental and environmental signals, exerting multi-layered regulatory effects on various secondary metabolic pathways including flavonoids [77]. Metabolomic analysis of transgenic *Loropetalum chinense* var. *rubrum* materials in this study revealed that in the anthocyanin metabolites, overexpression of *LcWRKY18* significantly reduced the contents of various anthocyanins such as cyanidin and delphinidin, while interference significantly increased the contents of peonidin and its derivatives. In proanthocyanidin metabolites, overexpression suppressed their accumulation, whereas interference promoted accumulation. These results reveal that *LcWRKY18* may exhibit differential regulatory functions on different branch pathways of flavonoids. Collectively, *LcWRKY18* likely exerts differential regulatory effects on anthocyanin and proanthocyanidin biosynthesis in *Loropetalum chinense* var. *rubrum*.

Promoter analysis showed that *LcPAL*, *LcANS* and *LcUFGT* contain W-box-related cis-elements, and dual-luciferase assays demonstrated that *LcWRKY18* significantly repressed the activities of these promoters. Together with the observed down-regulation of anthocyanin structural genes in transgenic materials, these results indicate that *LcWRKY18* may repress anthocyanin biosynthesis by acting upstream of key pathway genes. This inference is consistent with the well-established ability of WRKY proteins to bind W-box elements and regulate downstream transcription[36], although direct physical binding still requires further confirmation.

Abbreviations

ANS
anthocyanidin synthase
CHS
chalcone synthase
DFR
dihydroflavonol 4-reductase
GSA
Genome Sequence Archive
qRT-PCR
quantitative real-time PCR
RNA-seq
RNA sequencing
UFGT
UDP-glucose: flavonoid 3-O-glucosyltransferase
VIGS
virus-induced gene silencing
WRKY
WRKY transcription factor.

Declarations

Funding

This work was supported by the Natural Science Foundation of Hunan Province (2024JJ5178), the Natural Science Foundation of Changsha, Hunan Province (kq2402112), the Hunan Provincial Forestry Bureau (XLK202437), the Scientific Research Project of the Hunan Provincial Department of Education (24C1372), the Hunan Provincial Graduate Innovation Project (CX20240643 and CX20251094), the National Innovation and Entrepreneurship Training Program for College Students of China (S202310537005), the Yuelushan Laboratory Talent Program (2025RC3004), the Furong High-Level Talent Program (2025RC4005), and Hunan Agricultural University (25KJ021).

Author contributions

Anqi Huang, Mingtong Ren, and Lili Xiang contributed equally to this work. Anqi Huang, Mingtong Ren, Lili Xiang, Nan Ma, Xiaoying Yu, and Yanlin Li designed the study. Anqi Huang, Mingtong Ren, Lili Xiang, Yang Liu, Jiaxuan Li, Zhenkun Liao, and Lu Xu performed the experiments and collected the data. Anqi Huang, Mingtong Ren, Lili Xiang, and Donglin Zhang analyzed the data and interpreted the results. Nan Ma, Xiaoying Yu, and Yanlin Li supervised the research and acquired funding. Anqi Huang drafted the manuscript. All authors revised the manuscript and approved the final version.

Declaration of competing interest

The authors declare that they have no known competing financial interests or personal relationships that could have appeared to influence the work reported in this paper.

Ethics approval and consent to participate

Experimental research on plants, including the collection of plant materials, complied with relevant institutional, national and international guidelines and legislation. No specific permits were required for the cultivated plant materials used in this study.

Consent for publication

Not applicable.

Data availability

The RNA-seq datasets generated and analysed during the current study have been deposited in the Genome Sequence Archive (GSA) of the National Genomics Data Center, China National Center for Bioinformation. The heat-stress transcriptome datasets of *Loropetalum chinense* var. *rubrum* leaves have been submitted under BioProject accession number PRJCA063709 and GSA submission number subCRA069695. The transcriptome datasets of LcWRKY18 transgenic hairy roots have been submitted under BioProject accession number PRJCA063659 and GSA submission number subCRA069621. These datasets are currently under confidential status and will be released upon publication. The final GSA accession numbers will be updated after database processing and assignment.

Acknowledgements

The authors thank the Molecular Biology Technology Platform of Yuelushan Laboratory and the Hunan Mid-subtropical Quality Plant Breeding and Utilization Engineering Technology Research Center for technical support.

Graphical abstract text

Under high temperature, *LcWRKY18* is induced in red-leaved *Loropetalum chinense* var. *rubrum*. Elevated *LcWRKY18* suppresses the expression of key anthocyanin biosynthetic genes, including LcPAL, LcANS, and LcUFGT, leading to reduced anthocyanin accumulation and accelerated leaf regreening. Functional analyses using hairy root transformation, transcriptomics, metabolomics, and promoter activity assays support the role of *LcWRKY18* as a negative regulator of anthocyanin biosynthesis during high temperature.

References

The reference list from the original manuscript is retained below. Existing English entries are preserved, while Chinese entries are kept in their original form for accuracy.

1. Haque M, Tanjima U, Sushmoy D, et al. Heat stress alters chlorophyll fluorescence, photosynthesis and antioxidative enzyme activities in wheat cultivars[J]. Fundamental and Applied Agriculture, 2019(0): 1.
2. Liu Y, Lin L, Liu Y, et al. Genome-wide analysis of the bHLH gene family in loropetalum chinense var. rubrum: Identification, classification, evolution, and diversity of expression patterns under cultivation[J]. Plants, 2023, 12(19): 3392.
3. Liu Y, Lin L, Liu Y, et al. Genome-wide analysis of the bHLH gene family in loropetalum chinense var. rubrum : Identification, classification, evolution, and diversity of expression patterns under cultivation[J]. Plants, 2023, 12(19): 3392.
4. Zhang Y, Liu Y, Ling L, et al. Phenotypic, physiological, and molecular response of loropetalum chinense var. rubrum under different light quality treatments based on leaf color changes.[J]. Plants, 2023, 12(11): 2169.
5. Cai W, Zhang D, Zhang X, et al. Leaf color change and photosystem function evaluation under heat treatment revealed the stress resistance variation between loropetalum chinense and L. chinense var. rubrum.[J]. PeerJ, 2023, 11: e14834.
6. Kong J M, Chia L S, Goh N K, et al. Analysis and biological activities of anthocyanins[J]. Phytochemistry, 2003, 64(5): 923-933.
7. Winkel-Shirley B. Flavonoid biosynthesis. A colorful model for genetics, biochemistry, cell biology, and biotechnology[J]. Plant Physiology, 2001, 126(2): 485-493.
8. Cipollini M L, Levey D J. Secondary metabolites of fleshy vertebrate-dispersed fruits: Adaptive hypotheses and implications for seed dispersal[J]. American Naturalist, 1997, 150(3): 346-372.

9. Impact of low-temperature stress on general phenylpropanoid and anthocyanin pathways: enhancement of transcript abundance and anthocyanin pigmentation in maize seedlings | planta | springer nature link[EB/OL]. [2026-03-26]. https://link.springer.com/article/10.1007/BF00714468.
10. De Rosas I, Deis L, Baldo Y, et al. High temperature alters anthocyanin concentration and composition in grape berries of malbec, merlot, and pinot noir in a cultivar-dependent manner[J]. Plants, 2022, 11(7): 926.
11. Lo Piero A R, Puglisi I, Rapisarda P, et al. Anthocyanins accumulation and related gene expression in red orange fruit induced by low temperature storage[J]. Journal of Agricultural and Food Chemistry, 2005, 53(23): 9083-9088.
12. Treutter D. Significance of flavonoids in plant resistance and enhancement of their biosynthesis[J]. Plant Biology (Stuttgart, Germany), 2005, 7(6): 581-591.
13. Guo N, Cheng F, Wu J, et al. Anthocyanin biosynthetic genes in brassica rapa[J]. BMC Genomics, 2014, 15(1): 426.
14. Chen L, Hu B, Qin Y, et al. Advance of the negative regulation of anthocyanin biosynthesis by MYB transcription factors[J]. Plant Physiology and Biochemistry, 2019, 136: 178-187.
15. Tsuda T. Dietary anthocyanin-rich plants: Biochemical basis and recent progress in health benefits studies[J]. Molecular Nutrition & Food Research, 2012, 56(1): 159-170.
16. Transcriptomic and metabolomic analyses reveal that MYB transcription factors regulate anthocyanin synthesis and accumulation in the disc florets of the anemone form of chrysanthemum morifolium - ScienceDirect[EB/OL]. [2026-03-26]. https://www.sciencedirect.com/science/article/pii/S0304423821009547.
17. Gonzalez A, Zhao M, Leavitt J M, et al. Regulation of the anthocyanin biosynthetic pathway by the TTG1/bHLH/myb transcriptional complex in arabidopsis seedlings[J]. Plant Journal, 2008, 53(5): 814-827.
18. MdMYB114 regulates anthocyanin biosynthesis and functions downstream of MdbZIP4-like in Apple fruit - ScienceDirect[EB/OL]. [2026-03-26]. https://www.sciencedirect.com/science/article/pii/S0176161720302431.
19. Zhou B, Wang Y, Zhan Y, et al. Chalcone synthase family genes have redundant roles in anthocyanin biosynthesis and in response to blue/UV-a light in turnip (brassica rapa; brassicaceae)[J]. American Journal of Botany, 2013, 100(12): 2458-2467.
20. Heppel S C, Jaffé F W, Takos A M, et al. Identification of key amino acids for the evolution of promoter target specificity of anthocyanin and proanthocyanidin regulating MYB factors[J]. Plant Molecular Biology, 2013, 82(4-5): 457-471.
21. Duan S, Wang J, Gao C, et al. Functional characterization of a heterologously expressed brassica napus WRKY41-1 transcription factor in regulating anthocyanin biosynthesis in arabidopsis thaliana[J]. Plant Science, 2018, 268: 47-53.
22. Mao Z, Jiang H, Wang S, et al. The MdHY5-MdWRKY41-MdMYB transcription factor cascade regulates the anthocyanin and proanthocyanidin biosynthesis in red-fleshed apple[J]. Plant Science:

An International Journal of Experimental Plant Biology, 2021, 306: 110848.

23. Apple NAC transcription factor MdNAC52 regulates biosynthesis of anthocyanin and proanthocyanidin through MdMYB9 and MdMYB11 - ScienceDirect[EB/OL]. [2026-03-26]. https://www.sciencedirect.com/science/article/abs/pii/S0168945219308295.
24. Zhang S, Chen Y, Zhao L, et al. A novel NAC transcription factor, MdNAC42, regulates anthocyanin accumulation in red-fleshed apple by interacting with MdMYB10[J]. Tree Physiology, 2020, 40(3): 413-423.
25. Sun C, Wang C, Zhang W, et al. The R2R3-type MYB transcription factor MdMYB90-like is responsible for the enhanced skin color of an apple bud sport mutant[J]. Horticulture Research, 2021, 8(1): 156.
26. Sun C, Deng L, Du M, et al. A transcriptional network promotes anthocyanin biosynthesis in tomato flesh[J]. Molecular Plant, 2020, 13(1): 42-58.
27. Takos A M, Jaffé F W, Jacob S R, et al. Light-induced expression of a MYB gene regulates anthocyanin biosynthesis in red apples[J]. Plant Physiology, 2006, 142(3): 1216-1232.
28. Tao R, Bai S, Ni J, et al. The blue light signal transduction pathway is involved in anthocyanin accumulation in “red zaosu” pear[J]. Planta, 2018, 248(1): 37-48.
29. Bai S, Tao R, Tang Y, et al. BBX16, a B-box protein, positively regulates light-induced anthocyanin accumulation by activating MYB10 in red pear[J]. Plant Biotechnology Journal, 2019, 17(10): 1985-1997.
30. Eulgem T, Rushton P J, Robatzek S, et al. The WRKY superfamily of plant transcription factors[J]. Trends in Plant Science, 2000, 5(5): 199-206.
31. Chen F, Hu Y, Vannozzi A, et al. The WRKY transcription factor family in model plants and crops[J]. Critical Reviews in Plant Sciences, 2017, 36(5-6): 311-335.
32. Sun Y, Yu D. Activated expression of AtWRKY53 negatively regulates drought tolerance by mediating stomatal movement[J]. Plant Cell Reports, 2015, 34(8): 1295-1306.
33. Krishnamurthy P, Vishal B, Ho W J, et al. Regulation of a cytochrome P450 gene CYP94B1 by WRKY33 transcription factor controls apoplastic barrier formation in roots to confer salt tolerance. [J]. Plant Physiology, 2020, 184(4): 2199-2215.
34. Li S, Fu Q, Chen L, et al. Arabidopsis thaliana WRKY25, WRKY26, and WRKY33 coordinate induction of plant thermotolerance.[J]. Planta, 2011, 233(6): 1237-1252.
35. Zou C, Jiang W, Yu D. Male gametophyte-specific WRKY34 transcription factor mediates cold sensitivity of mature pollen in Arabidopsis.[J]. Journal of Experimental Botany, 2010, 61(14): 3901-3914.
36. Han M, Kim C Y, Lee J, et al. OsWRKY42 represses OsMT1d and induces reactive oxygen species and leaf senescence in rice.[J]. Molecules and Cells, 2014, 37(7): 532-539.
37. Zhang M, Zhao R, Huang K, et al. The OsWRKY63-OsWRKY76-OsDREB1B module regulates chilling tolerance in rice.[J]. Plant Journal, 2022, 112(2): 383-398.

38. Cai R, Dai W, Zhang C, et al. The maize WRKY transcription factor ZmWRKY17 negatively regulates salt stress tolerance in transgenic arabidopsis plants.[J]. Planta, 2017, 246(6): 1215-1231.
39. Zhang L, Cheng J, Sun X, et al. Overexpression of VaWRKY14 increases drought tolerance in arabidopsis by modulating the expression of stress-related genes.[J]. Plant Cell Reports, 2018, 37(8): 1159-1172.
40. Xu P yue, Xu L, Xu H feng, et al. MdWRKY40is directly promotes anthocyanin accumulation and blocks MdMYB15L, the repressor of MdCBF2, which improves cold tolerance in apple[J]. Journal of Integrative Agriculture, 2023, 22(6): 1704-1719.
41. Su M, Wang S, Li C, et al. Ultraviolet-B-induced MdWRKY71-L expression regulates anthocyanin synthesis in apple[J]. Environmental and Experimental Botany, 2022, 201: 105000.
42. Ma H, Yang T, Li Y, et al. The long noncoding RNA MdLNC499 bridges MdWRKY1 and MdERF109 function to regulate early-stage light-induced anthocyanin accumulation in apple fruit[J]. The Plant Cell, 2021, 33(10): 3309-3330.
43. Alabd A, Ahmad M, Zhang X, et al. Light-responsive transcription factor PpWRKY44 induces anthocyanin accumulation by regulating PpMYB10 expression in pear[J]. Horticulture Research, 2022, 9: uhac199.
44. Bi M, Liang R, Wang J, et al. Multifaceted roles of LhWRKY44 in promoting anthocyanin accumulation in asiatic hybrid lilies (lilium spp.)[J]. Horticulture Research, 2023, 10(9): uhad167.
45. Liu Y, Zhang Y, Liu Y, et al. Genome-wide identification and characterization of WRKY transcription factors and their expression profile in loropetalum chinense var. rubrum.[J]. Plants, 2023, 12(11): 2131.
46. Chen C, Chen H, Zhang Y, et al. TBtools: An integrative toolkit developed for interactive analyses of big biological data[J]. Molecular Plant, 2020, 13(8): 1194-1202.
47. Adasme M F, Linnemann K L, Bolz S N, et al. PLIP 2021: Expanding the scope of the protein-ligand interaction profiler to DNA and RNA[J]. Nucleic Acids Research, 2021, 49(W1): W530-W534.
48. Wen C, Zhang Z, Shi Q, et al. Methyl jasmonate- and salicylic acid-induced transcription factor ZjWRKY18 regulates triterpenoid accumulation and salt stress tolerance in jujube[J]. International Journal of Molecular Sciences, 2023, 24(4).
49. Ishiguro S, Nakamura K. Characterization of a cDNA encoding a novel DNA-binding protein, SPF1, that recognizes SP8 sequences in the 5' upstream regions of genes coding for sporamin and beta-amylase from sweet potato[J]. Molecular & general genetics: MGG, 1994, 244(6): 563-571.
50. Ulker B, Somssich I E. WRKY transcription factors: From DNA binding towards biological function[J]. Current Opinion in Plant Biology, 2004, 7(5): 491-498.
51. Ross C A, Liu Y, Shen Q J. The WRKY gene family in rice (oryza sativa)[J]. Journal of Integrative Plant Biology, 2007, 49(6): 827-842.
52. Wei K F, Chen J, Chen Y F, et al. Molecular phylogenetic and expression analysis of the complete WRKY transcription factor family in maize.[J]. DNA Research, 2012, 19(2): 153-164.

53. Zhou C, Lin Q, Lan J, et al. WRKY transcription factor OsWRKY29 represses seed dormancy in rice by weakening abscisic acid response[J]. Frontiers in Plant Science, 2020, 11: 691.
54. Jiang W, Yu D. Arabidopsis WRKY2 transcription factor mediates seed germination and postgermination arrest of development by abscisic acid[J]. BMC Plant Biology, 2009, 9(1): 96.
55. Hu Z, Wang R, Zheng M, et al. TaWRKY51 promotes lateral root formation through negative regulation of ethylene biosynthesis in wheat (triticum aestivum L.)[J]. The Plant Journal: For Cell and Molecular Biology, 2018, 96(2): 372-388.
56. Grunewald W, De Smet I, Lewis D R, et al. Transcription factor WRKY23 assists auxin distribution patterns during *arabidopsis* root development through local control on flavonol biosynthesis[J]. Proceedings of the National Academy of Sciences, 2012, 109(5): 1554-1559.
57. Wang P, Xu X, Tang Z, et al. OsWRKY28 regulates phosphate and arsenate accumulation, root system architecture and fertility in rice[J]. Frontiers in Plant Science, 2018, 9: 1330.
58. Lei R, Li X, Ma Z, et al. Arabidopsis WRKY2 and WRKY34 transcription factors interact with VQ20 protein to modulate pollen development and function[J]. The Plant Journal: For Cell and Molecular Biology, 2017, 91(6): 962-976.
59. Li W, Wang H, Yu D. Arabidopsis WRKY transcription factors WRKY12 and WRKY13 oppositely regulate flowering under short-day conditions[J]. Molecular Plant, 2016, 9(11): 1492-1503.
60. Cheng Z, Luan Y, Meng J, et al. WRKY transcription factor response to high-temperature stress[J]. Plants (Basel, Switzerland), 2021, 10(10): 2211.
61. Zhang Y, Wang L. The WRKY transcription factor superfamily: Its origin in eukaryotes and expansion in plants[J]. BMC Evolutionary Biology, 2005, 5: 1.
62. Berri S, Abbruscato P, Faivre-Rampant O, et al. Characterization of WRKYco-regulatory networks in rice and Arabidopsis[J]. BMC Plant Biology, 2009, 9(1): 120.
63. Blanc G, Hokamp K, Wolfe K H. A recent polyploidy superimposed on older large-scale duplications in the *arabidopsis* genome[J]. Genome Research, 2003, 13(2): 137-144.
64. Wu K L, Guo Z J, Wang H H, et al. The WRKY family of transcription factors in rice and arabidopsis and their origins[J]. DNA research: an international journal for rapid publication of reports on genes and genomes, 2005, 12(1): 9-26.
65. Xu S, Feng H, Li T, et al. Genome-wide analysis of the *WRKY* gene family in lily and functional characterization of *LdWRKY87* in response to heat stress[J]. New Crops, 2026, 3: 100084.
66. Khan I, Lubna, Bilal S, et al. Genome-wide and transcriptome analysis of PdWRKY transcription factors in date palm (Phoenix dactylifera) revealing insights into heat and drought stress tolerance[J]. BMC Genomics, 2025, 26(1): 589.
67. Zhu X, Duan X, Majeed Y, et al. Functional analysis of StWRKY75 gene in response to heat stress in potato (solanum tuberosum L.)[J]. Frontiers in Plant Science, 2025, 16.
68. Nakashima K, Yamaguchi-Shinozaki K, Shinozaki K. The transcriptional regulatory network in the drought response and its crosstalk in abiotic stress responses including drought, cold, and heat[J].

Frontiers in Plant Science, 2014, 5.

69. Wang J, Zhang X, Wang G. Transcriptomic analysis of heat-responsive genes in maize seedlings[J]. Maize Genomics and Genetics, 2025, 16(0).
70. Li C, Wu J, Hu K D, et al. PyWRKY26 and PybHLH3 cotargeted the PyMYB114 promoter to regulate anthocyanin biosynthesis and transport in red-skinned pears[J]. Horticulture Research, 2020, 7: 37.
71. Peng Y, Thrimawithana A H, Cooney J M, et al. The proanthocyanin-related transcription factors MYBC1 and WRKY44 regulate branch points in the kiwifruit anthocyanin pathway[J]. Scientific Reports, 2020, 10(1): 14161.
72. Wang Y qiao, Zhao X jie, Niu F fang, et al. Analysis of transcriptional activity and interaction proteins of WRKY31 transcription factor in arabidopsis thaliana[J]. Biotechnology Bulletin, 2018, 34(5): 101.
73. Ma A, Li J, Liu S, et al. WRKY61 negatively regulates aluminum resistance by inhibiting the expression of ALMT1 in arabidopsis thaliana[J]. Plants, 2025, 14(21).
74. Bi M, Xu L, Wang J, et al. Three transcription factors form an activation-inhibition module to regulate anthocyanin accumulation in asiatic hybrid lilies[J]. Plant Physiology, 2025, 198(2): kiaf203.
75. Tak H, Negi S, Ganapathi T R. The 5'-upstream region of WRKY18 transcription factor from banana is a stress-inducible promoter with strong expression in guard cells[J]. Physiologia Plantarum, 2021, 173(4): 1335-1350.
76. Chen L, Cheng Y, Hong G. Molecular insights into the regulation of flavonoid biosynthesis in fruits[J]. Horticulture Research, 2026, 13(2): uhaf306.
77. Li Y, Li Z, Xu C, et al. WRKYs as regulatory hubs of secondary metabolic networks: Diverse inducers and distinct responses[J]. Plant Communications, 2025, 6(9): 101438.

Figures

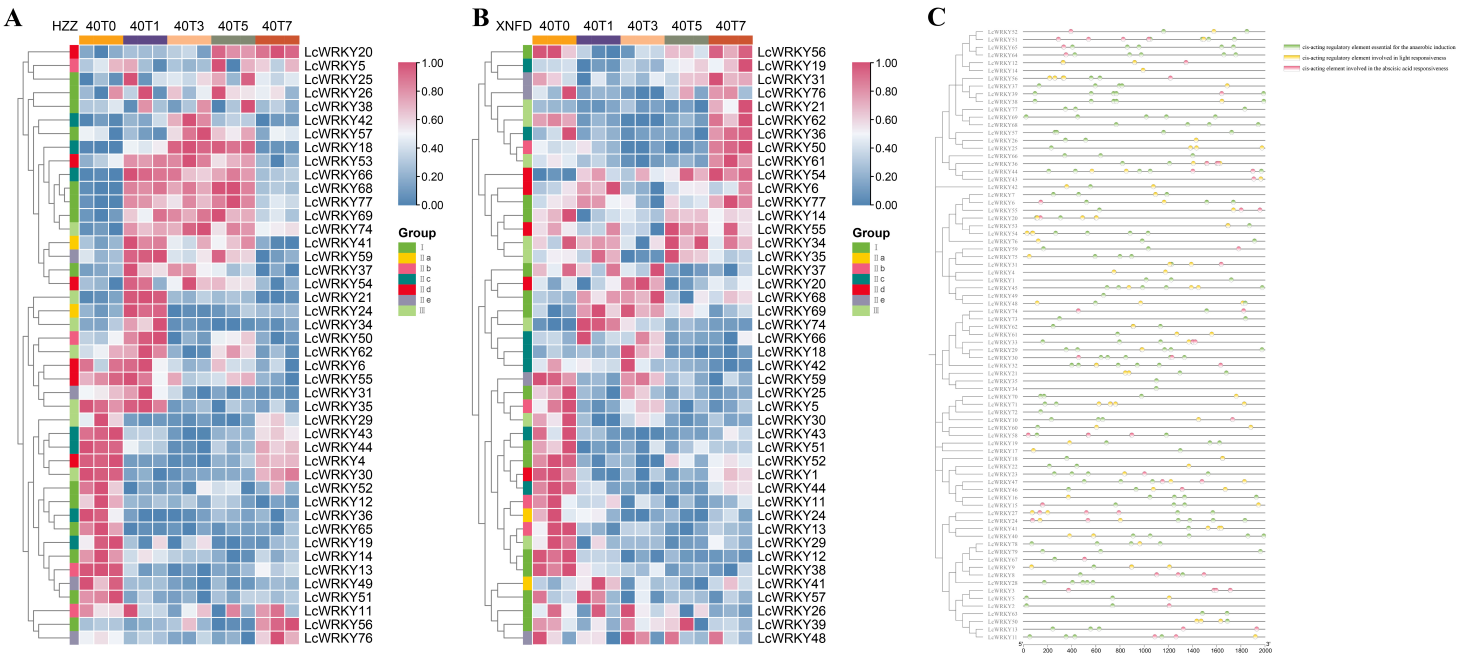


Figure 1

Expression profiles of *LcWRKY* family genes under high temperature. (A) High temperature showing the expression pattern of *LcWRKY*genes in ‘Hei Zhenzhu’. (B) High temperature showing the expression pattern of *LcWRKY* genes in ‘Xiangnong Fendai’.(C) Distribution of high temperature response elements in *LcWRKY*

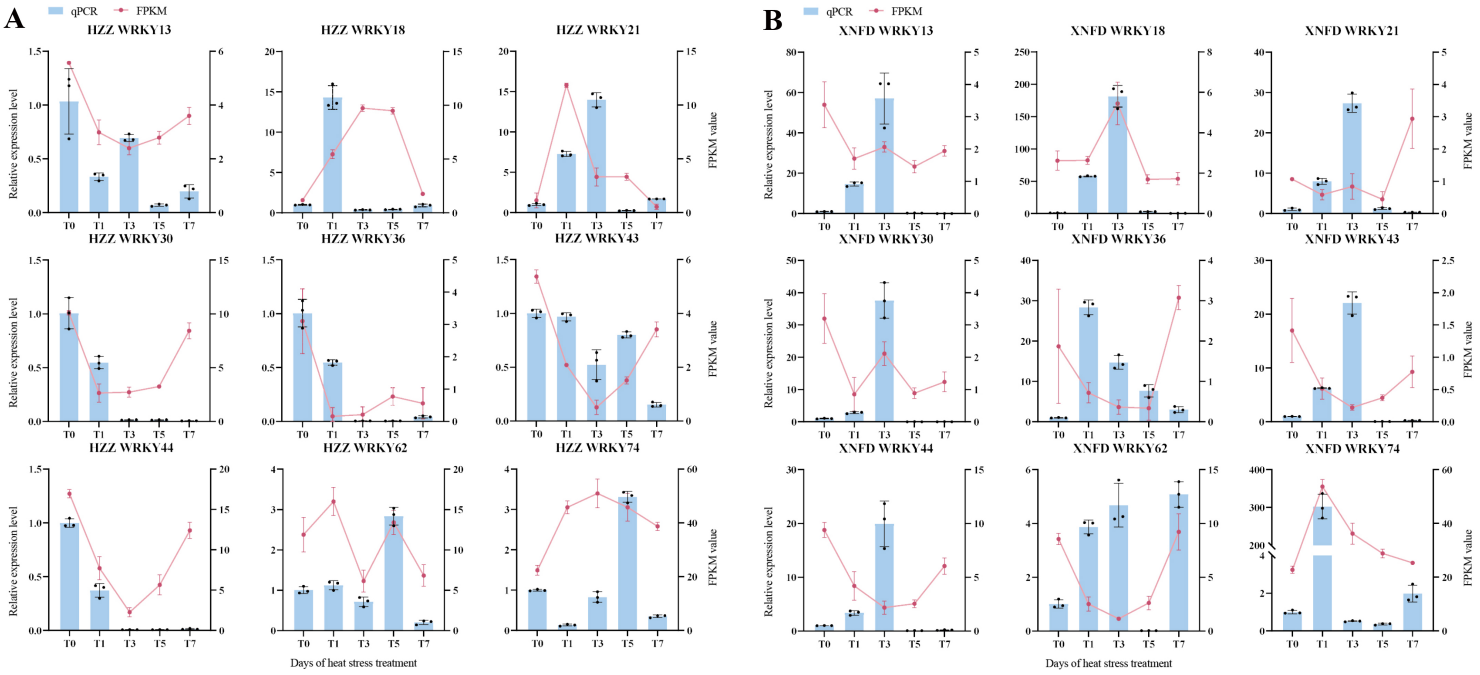


Figure 2

qRT-PCR validation of candidate high temperature *LcWRKY* genes. (A) Expression patterns in ‘Hei Zhenzhu’. (B) Expression patterns in ‘Xiangnong Fendai’. Data are presented as mean +- SD of three biological replicates.

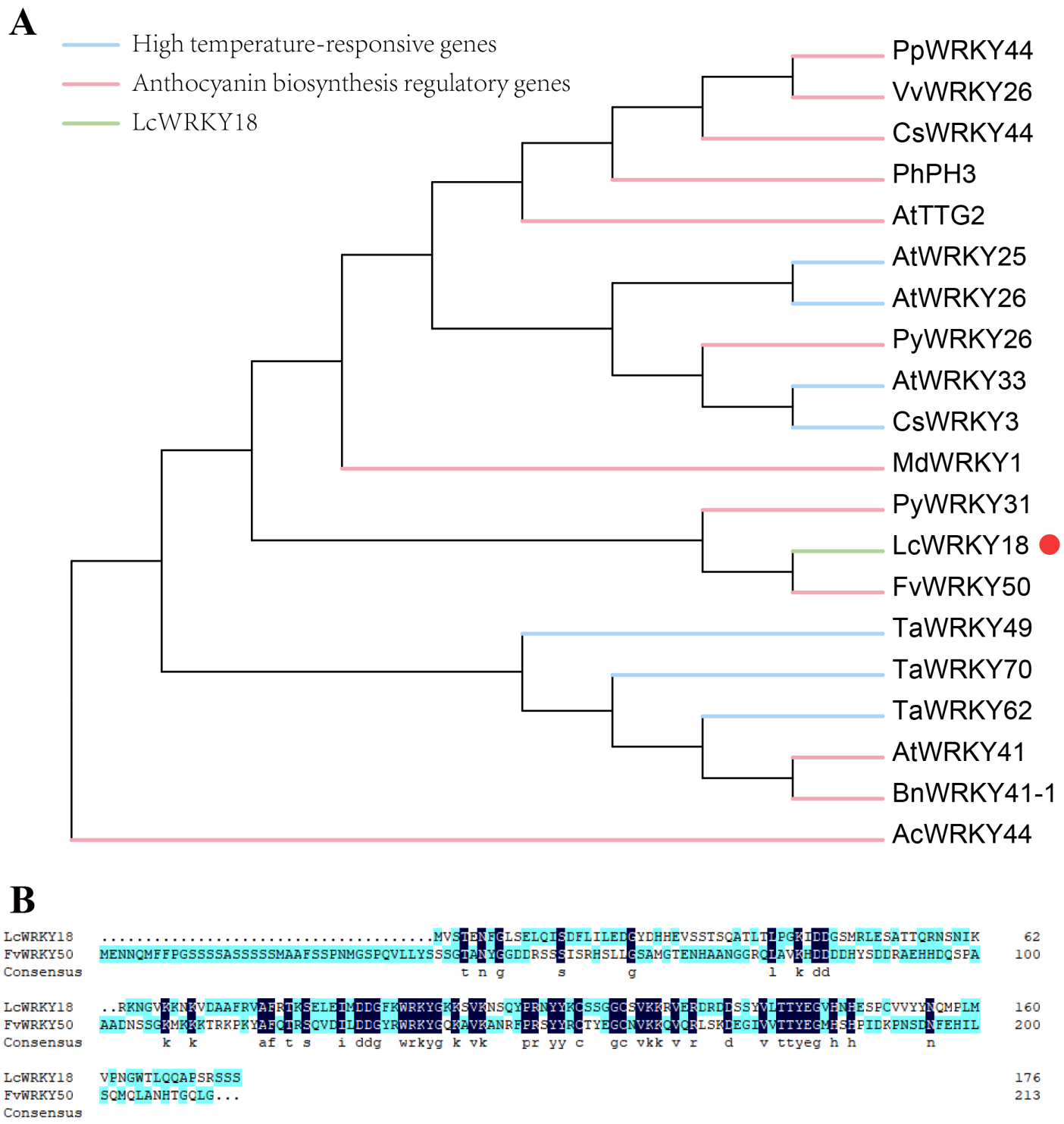


Figure 3

Bioinformatic analysis of *LcWRKY18*. (A) Phylogenetic relationship between *LcWRKY18* and representative WRKY proteins from other plant species. (B) Multiple sequence alignment of *LcWRKY18* and FvWRKY50.

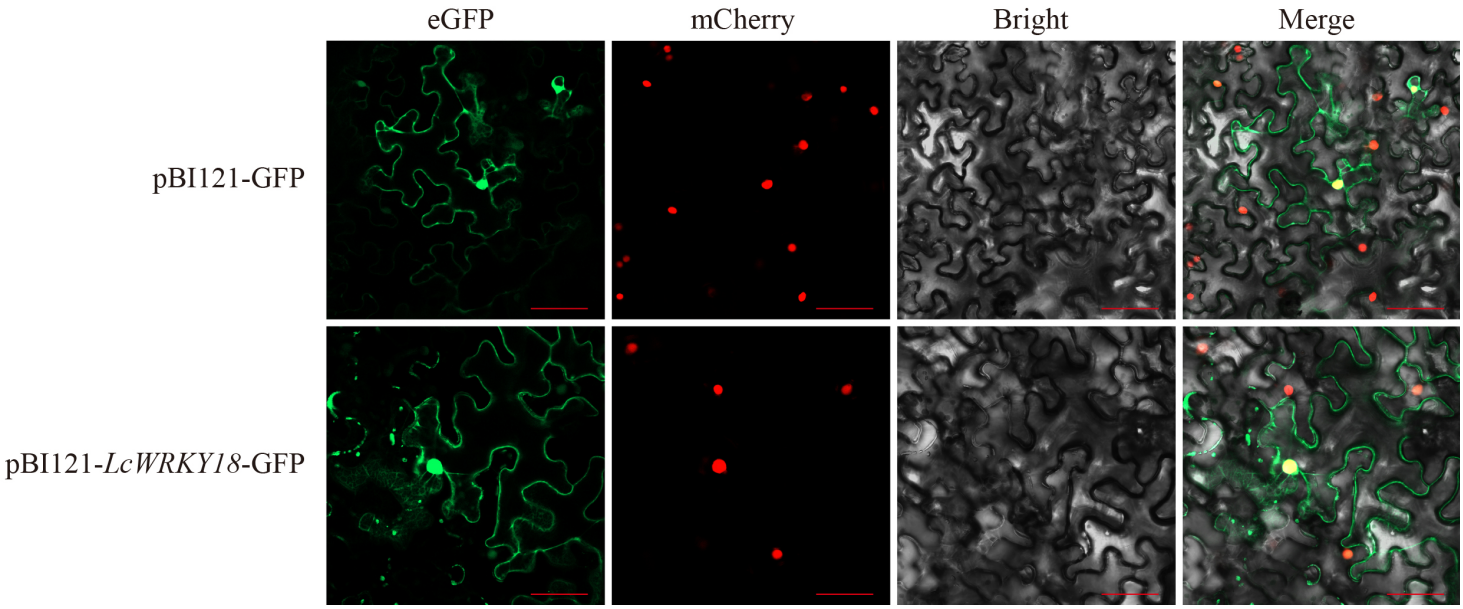


Figure 4

Subcellular localization of *LcWRKY18* in Nicotiana benthamiana epidermal cells.

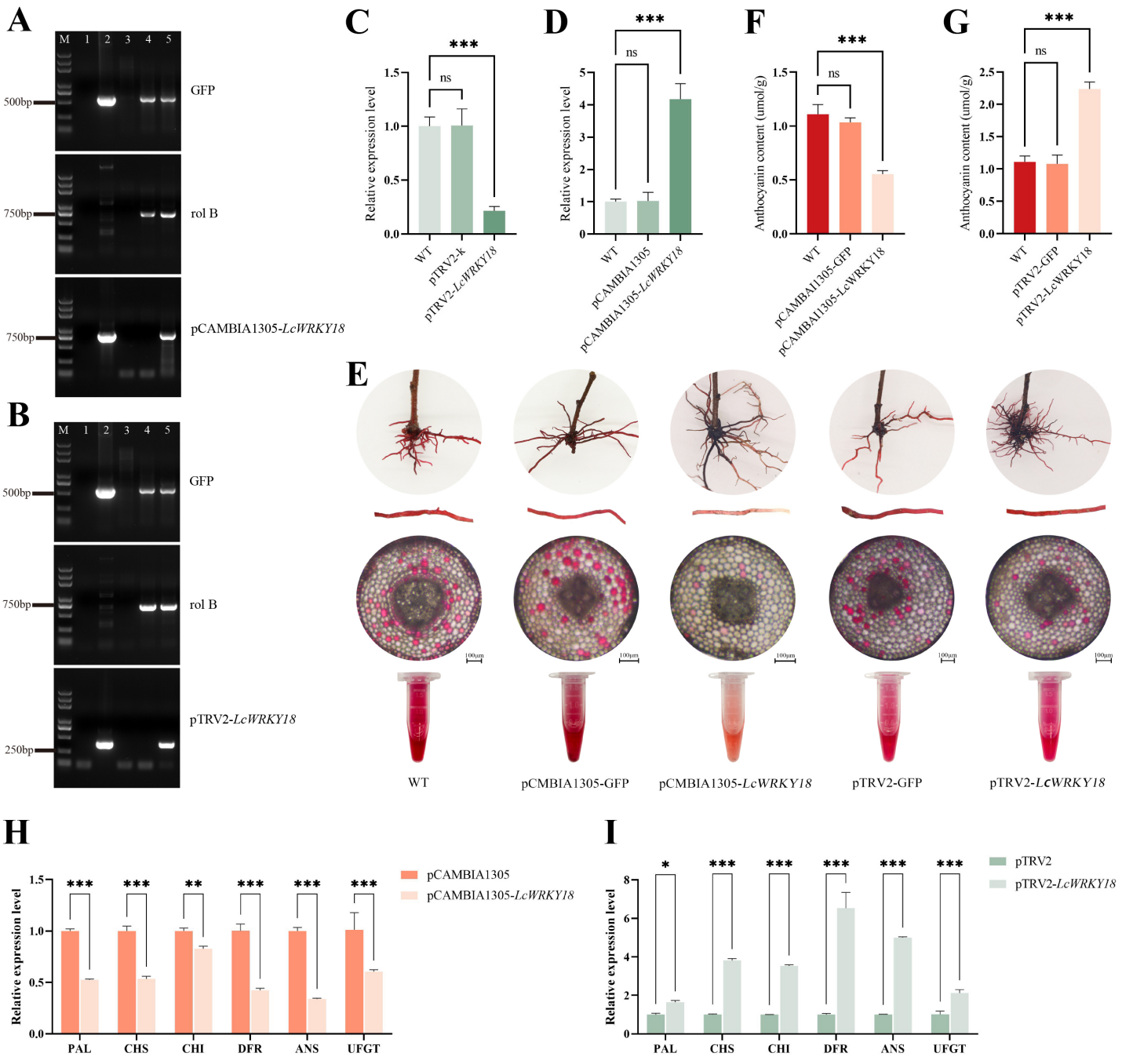


Figure 5

Molecular identification of transgenic hairy roots in *Loropetalum chinense* var. *rubrum*. (A) PCR verification of pCAMBIA1305-*LcWRKY18* transgenic roots in ‘Hei Zhenzhu’. (B) PCR verification of pTRV2-*LcWRKY18* transgenic roots in ‘Hei Zhenzhu’. (C) Relative expression levels of *LcWRKY18*in overexpression and interference lines. (D) Phenotypes of transgenic roots. (E) Microscopic observation of root pigmentation. (F) Anthocyanin content of different root lines. Different lowercase letters indicate significant differences at P < 0.05.（H）Expression Levels of Anthocyanin Biosynthetic Structural Genes in Roots Transformed with pCAMBIA1305-*LcWRKY18*. (I) Expression Levels of Anthocyanin Biosynthetic Structural Genes in Roots Transformed with pTRV2-*LcWRKY18*.

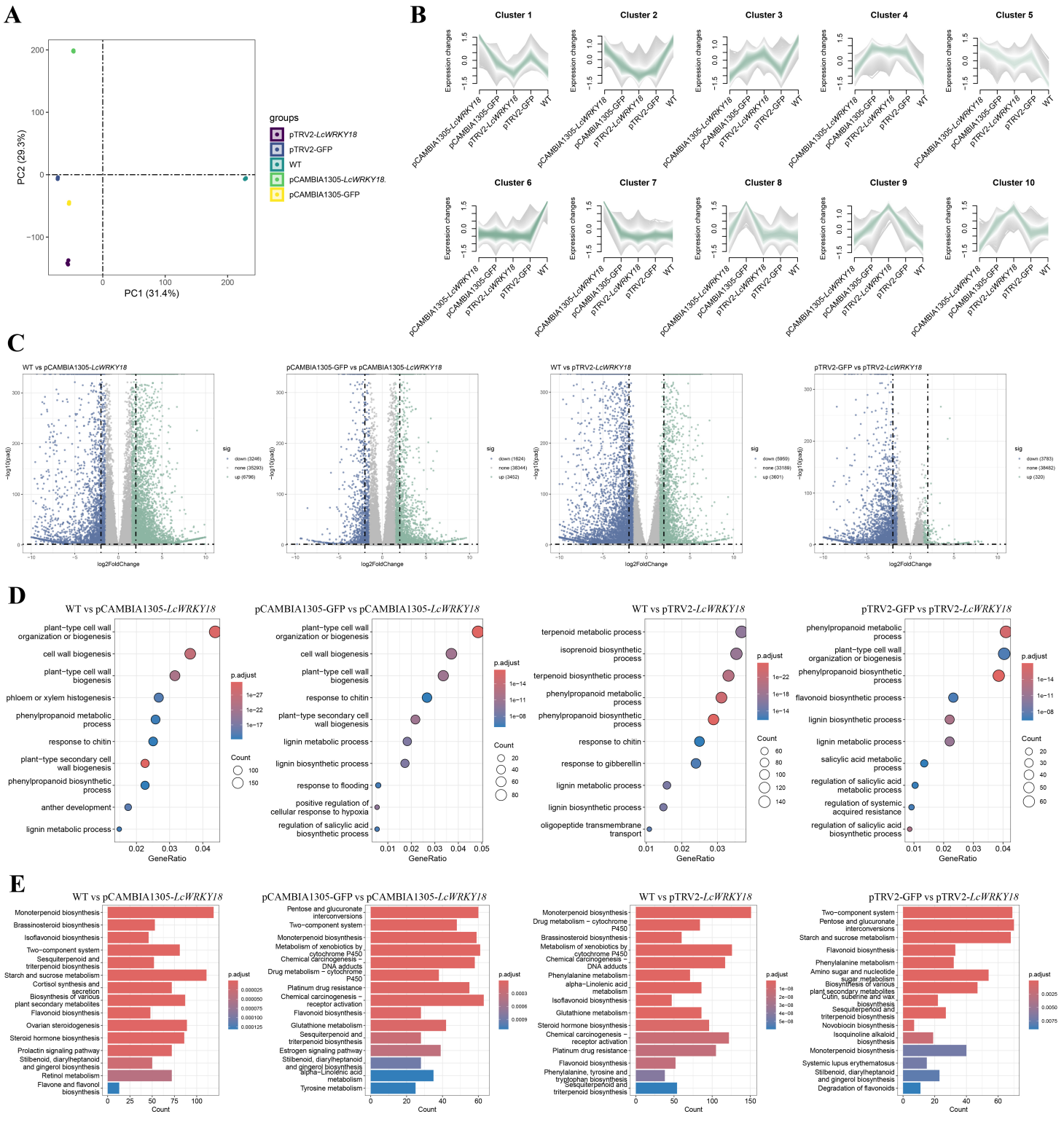


Figure 6

Transcriptomic analysis of *LcWRKY18* transgenic materials. (A) Principal component analysis of different sample groups. (B) Trend analysis of differentially expressed genes. (C) Volcano plots of differentially expressed genes among comparisons. (D) GO enrichment analysis of differentially expressed genes. (E) KEGG enrichment analysis of differentially expressed genes.

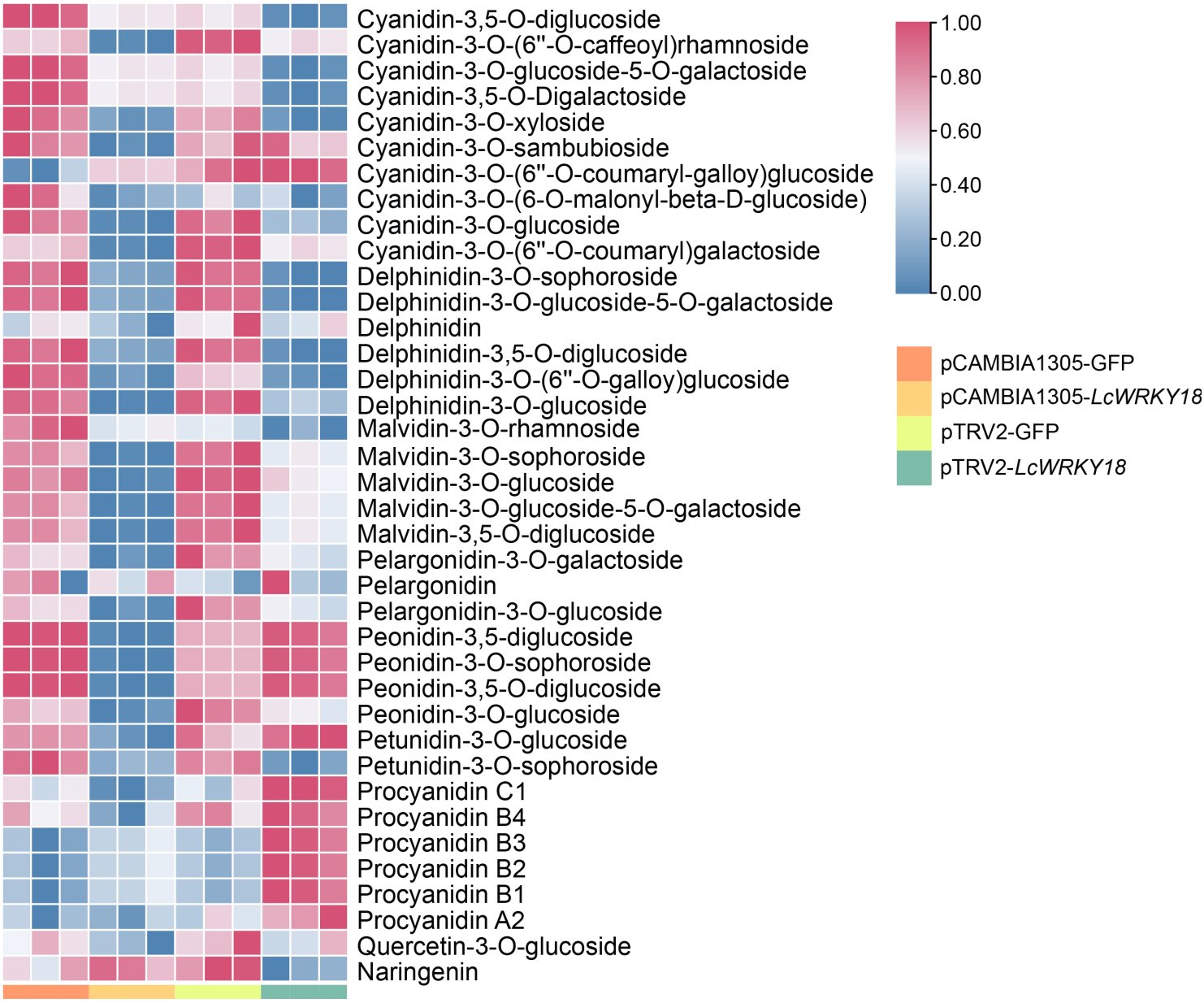


Figure 7

Heat map of anthocyanin metabolites detected in different transgenic root materials.

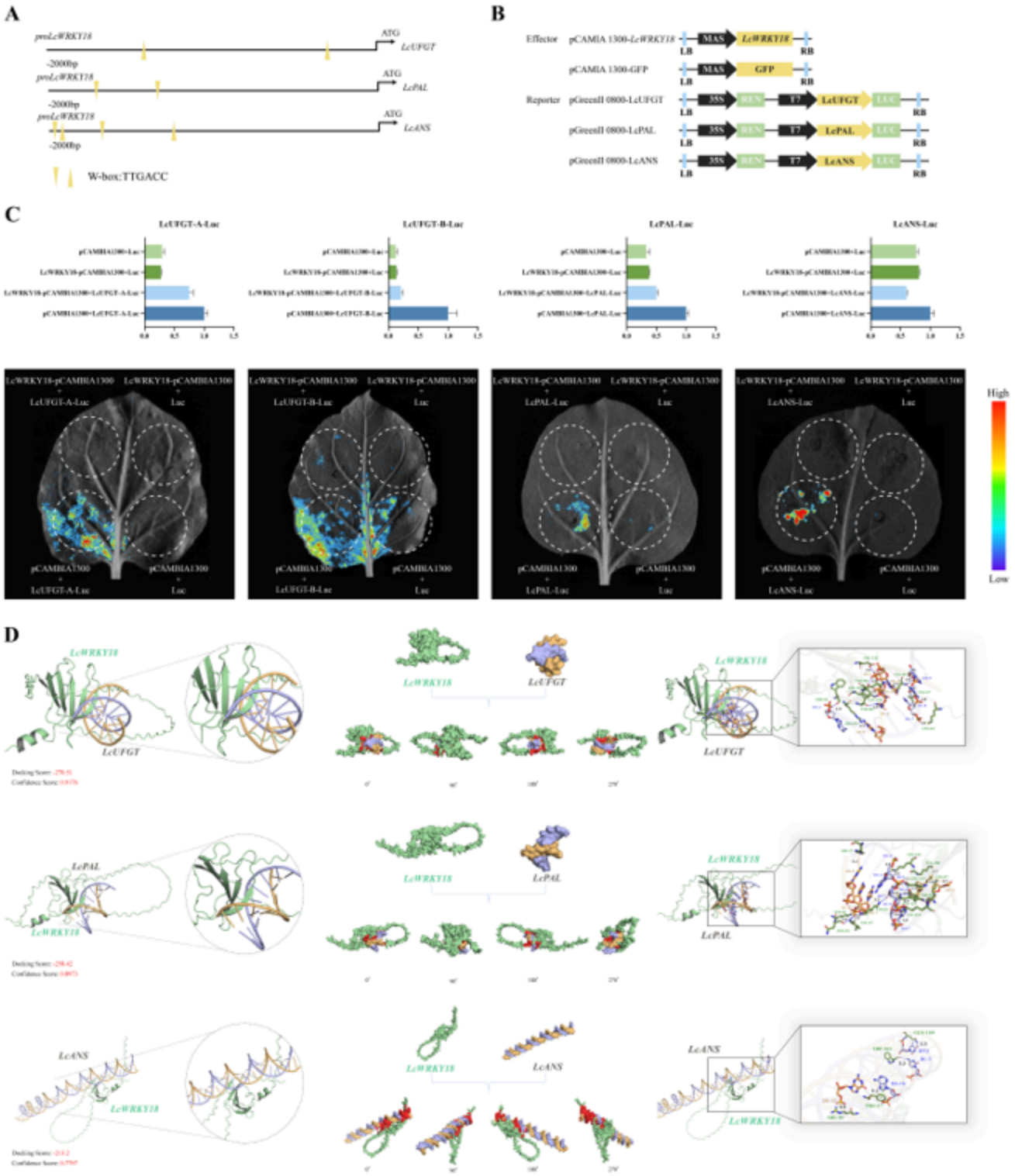


Figure 8

LcWRKY18 represses the promoter activities of key anthocyanin biosynthetic genes. (A) Schematic diagrams of the promoters of *LcUFGT*, *LcPAL* and *LcANS*. (B-D) Dual-luciferase assay results showing the effects of *LcWRKY18* on the activities of the three promoters. Different lowercase letters indicate significant differences at $P < 0.05$.

Supplementary Files

This is a list of supplementary files associated with this preprint. Click to download.

- SupplementaryFig1.jpg
- SupplementaryFig2.jpg
- SupplementaryFig3.jpg
- SupplementaryFig4.jpg
- SupplementaryFig5.jpg
- Fulllengthoriginalgelimages.pdf